LETTERS

Hidden magnetism and quantum criticality in the heavy fermion superconductor $CeRhIn_5$

Tuson Park[1], F. Ronning[1], H. Q. Yuan[2], M. B. Salamon[2], R. Movshovich[1], J. L. Sarrao[1] & J. D. Thompson[1]

With only a few exceptions that are well understood, conventional superconductivity does not coexist with long-range magnetic order (for example, ref. 1). Unconventional superconductivity, on the other hand, develops near a phase boundary separating magnetically ordered and magnetically disordered phases[2,3]. A maximum in the superconducting transition temperature T_c develops where this boundary extrapolates to zero Kelvin, suggesting that fluctuations associated with this magnetic quantum-critical point are essential for unconventional superconductivity[4,5]. Invariably, though, unconventional superconductivity masks the magnetic phase boundary when $T < T_c$, preventing proof of a magnetic quantum-critical point[5]. Here we report specific-heat measurements of the pressure-tuned unconventional superconductor $CeRhIn_5$ in which we find a line of quantum–phase transitions induced inside the superconducting state by an applied magnetic field. This quantum-critical line separates a phase of coexisting antiferromagnetism and superconductivity from a purely unconventional superconducting phase, and terminates at a quantum tetracritical point where the magnetic field completely suppresses superconductivity. The $T \rightarrow 0$ K magnetic field–pressure phase diagram of $CeRhIn_5$ is well described with a theoretical model[6,7] developed to explain field-induced magnetism in the high-T_c copper oxides, but in which a clear delineation of quantum–phase boundaries has not been possible. These experiments establish a common relationship among hidden magnetism, quantum criticality and unconventional superconductivity in copper oxides and heavy-electron systems such as $CeRhIn_5$.

$CeRhIn_5$ belongs to a family of cerium-, uranium- and plutonium-based compounds in which interactions between electrons enhance the effective mass of charge carriers up to 1,000 times the mass of a free electron. These heavy-electron materials in turn belong to a larger family of strongly correlated electron systems that includes the high-T_c copper oxide superconductors and some organic compounds. A generic temperature-control parameter (T–δ) phase diagram common to strongly correlated unconventional superconductors is shown in Fig. 1 (refs 5, 8–10). $CeRhIn_5$ is prototypical of this phase diagram, in this case with pressure as the tuning parameter[11,12]. At atmospheric pressure, $CeRhIn_5$ orders antiferromagnetically at 3.8 K, and with applied pressure the antiferromagnetic (AFM) state vanishes at $P_{c1} = 1.77$ GPa when the Néel temperature T_N equals the superconducting transition temperature $T_c = 1.9$ K. Over a range of pressures below P_{c1}, extensive measurements show[12–15] that magnetic order coexists with superconductivity, but only when $T_N > T_c$. Above P_{c1}, where $T_c > T_N$ (extrapolated), these measurements find only unconventional superconductivity. A smooth extrapolation of $T_N(P)$ to $T = 0$ K suggests that Néel order, if it existed, would terminate at a quantum critical point P_{c2} near 2.3 GPa, where the effective mass of charge carriers diverge in the normal state[16].

Figure 2 summarizes field-dependent specific-heat measurements on a single crystal of $CeRhIn_5$ subjected to pressures just below and above P_{c1}. For $P = 1.68$ GPa $< P_{c1}$ (Fig. 2a), these data confirm earlier conclusions[12–18] that an AFM order coexists with the superconducting phase. Above P_{c1} (Fig. 2b), only a specific-heat discontinuity due to superconductivity is observed for fields up to 44 kOe: there is no evidence for a magnetic phase transition at these low fields, consistent with other measurements at zero applied field[12–15,19]. At 55 kOe, a specific-heat anomaly near 0.7 K emerges below the superconducting transition ($T_c = 1.7$ K) and grows in intensity with increasing field. Finally, in Fig. 2c ($P = 2.3$ GPa), there is no signature for a magnetic transition up to 88 kOe and down to 300 mK. As the superconducting transition is suppressed to zero, the ratio between

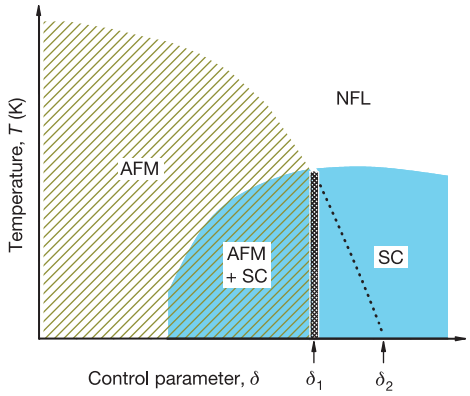

Figure 1 | Schematic temperature–control parameter (T–δ) phase diagram common to classes of unconventional superconductors. The hatched area represents an AFM state and the coloured area represents a superconducting (SC) phase. The hatched area in the coloured background denotes coexisting AFM and SC phases. In the normal state above the SC dome, physical properties are not typical of a metal and reflect non-Fermi liquid (NFL) behaviours. As the control parameter, such as chemical substitution or pressure is varied, long-range magnetic order gives way to a superconducting state. Above the superconducting dome, normal state properties are dominated by long-ranged, long-lived fluctuations that are expected if the magnetic phase boundary extended smoothly to absolute zero temperature, that is, to a magnetic quantum critical point (δ_2). Experimentally, however, magnetic order abruptly disappears at a finite temperature where the superconductivity and magnetic phase boundaries meet, suggesting a first-order or weakly first-order boundary at δ_1 and providing no obvious connection between magnetism and the putative δ_2. In such a case, it is difficult to reconcile the existence of an extended range of unconventional superconductivity beyond δ_1 and of an unusual normal state above T_c.

[1]Los Alamos National Laboratory, Los Alamos, New Mexico 87545, USA. [2]Department of Physics, University of Illinois at Urbana-Champaign, Urbana, Illinois 61801, USA.

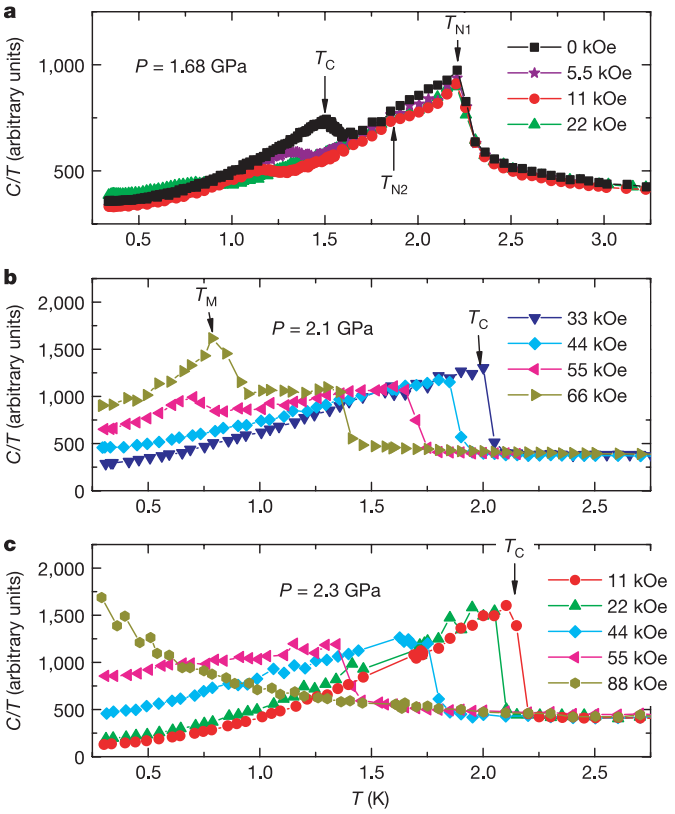

Figure 2 | Specific heat divided by temperature as a function of temperature for $CeRhIn_5$ at fixed magnetic fields. The magnetic field is applied perpendicular to the *c* axis of this tetragonal compound. Specific heat is determined by an alternating-current calorimetric method (see Supplementary Methods). **a**, At 1.68 GPa, specific-heat anomalies due to AFM transitions T_{N1} and T_{N2} and a superconducting transition T_c are observed. T_{N1} signals the onset of incommensurate antiferromagnetism with propagation wave vector (0.5, 0.5, 0.297) (ref. 17) and $T_{N2} = 1.85$ K is due to a spin reorientation transition[18]. As at atmospheric pressure, T_{N1} and T_{N2} are almost independent of the applied field. A specific-heat discontinuity due to superconductivity follows at 1.55 K. **b**, At 2.1 GPa, only a superconducting anomaly appears for $H \leq 44$ kOe (diamonds). At 55 kOe (side triangles), however, magnetism appears for $T < T_c(H)$. With further increasing field, the magnetic anomaly at T_M is enhanced and persists for $T > T_c(H)$, as shown in Supplementary Fig. 1. **c**, At 2.3 GPa, only superconductivity appears and magnetism is absent for $H \leq 88$ kOe and $T > 300$ mK.

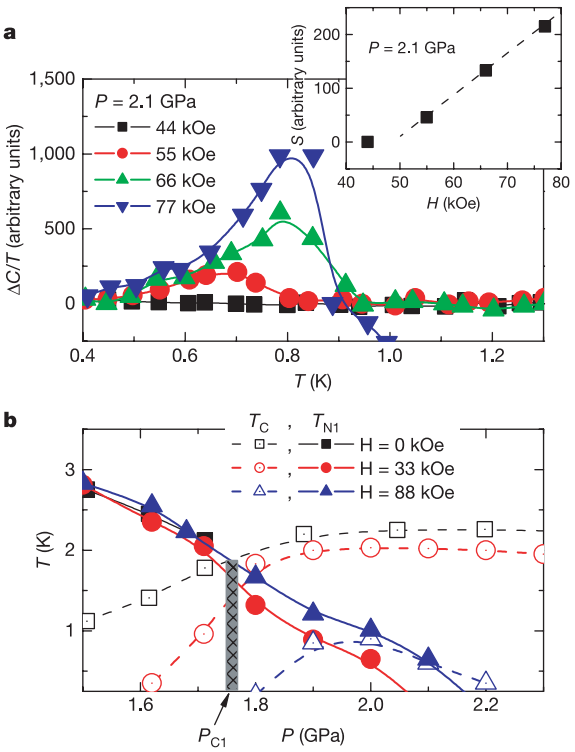

Figure 3 | Measurements of field and pressure dependence. a, Field-dependence of the magnetic specific heat of $CeRhIn_5$ at 2.1 GPa. To estimate the magnetic contribution to the specific heat $\Delta C/T$ due to magnetic order, we assume a smoothly varying background ($\sim T^2$) over a temperature range of interest and subtract that background contribution from the total measured specific heat. Inset, Entropy involved in the magnetic ordering transition, that is, area under the peak in $\Delta C/T$, as a function of magnetic field. The dashed line is a guide to eyes. The relative entropy associated with magnetic order is much less for $P = 2.1$ GPa than at $P = 0$ for any H. **b**, Temperature–pressure diagram at $H = 0$ kOe (squares), 33 kOe (circles), and 88 kOe (triangles). The magnetic transition is depicted as solid symbols and the superconducting transition by open symbols. Lines are spline fits to the data points.

specific heat and temperature C/T diverges weakly with decreasing temperature.

Figure 3a shows the evolution of the field-induced magnetic anomaly in C/T for $P = 2.1$ GPa. Similar results were obtained at $P = 1.8$ and 1.9 GPa, even closer to P_{c1}. The area under these curves is a measure of magnetic entropy (Fig. 3a inset) and reflects approximately the magnitude of the field-induced magnetism. The near-linear proportionality of the entropy to the applied field suggests that magnetism is associated with quantized vortices of magnetic flux that penetrate the superconductor and whose areal density is proportional to magnetic-field strength H. The H-induced transition temperature increases with H, consistent with the intrinsic magnetism, not with superconducting nor extrinsic phases. An explanation for these observations is discussed later.

A temperature–pressure phase diagram constructed from specific-heat measurements is plotted in Fig. 3b for representative fixed fields. For zero magnetic field, evidence for a magnetic transition temperature abruptly disappears at P_{c1}, suggesting a first-order-like transition. In an applied field of 33 kOe, however, the line of second-order magnetic transition temperatures T_{N1} smoothly evolves through P_{c1} and deep into the superconducting dome. With increasing field, the relative position of the critical points where T_{N1} becomes zero changes with respect to the centre of the superconducting dome. The influence of superconductivity on the development of magnetic order is reflected in a slope change of the magnetic transition line as it crosses into the superconducting domain.

These results are shown in Fig. 4 as a temperature–pressure–field phase diagram. The vertical field–pressure plane at a fixed temperature of 0.65 K changes very little with decreasing temperature to 350 mK, and we take it to be representative of a $T = 0$ K plane (see Supplementary Fig. 1). With increasing pressure, the magnetic field required to induce magnetism increases and finally meets the upper critical field line H_{c2} at $P_{c2} = 2.25$ GPa, a tetracritical point that branches out a transition line between magnetically ordered and disordered phases for $H > H_{c2}$. This observation of the H-induced magnetism only for $P_{c1} < P < P_{c2}$ now provides an explanation for the de Haas–van Alphen observation[16] of a diverging effective mass due to a field- and pressure-tuned quantum critical point at P_{c2}. At this pressure, the Fermi surface volume expands to accommodate additional delocalized charge carriers. The larger Fermi surface volume of $CeRhIn_5$ beyond P_{c2} corresponds closely to that of the isostructural superconductor $CeCoIn_5$ whose 4*f* electron from cerium contributes to the Fermi surface volume[16]. A localized to delocalized transition in the 4*f*-electron configuration is expected in a model of criticality in which extended and localized fluctuations

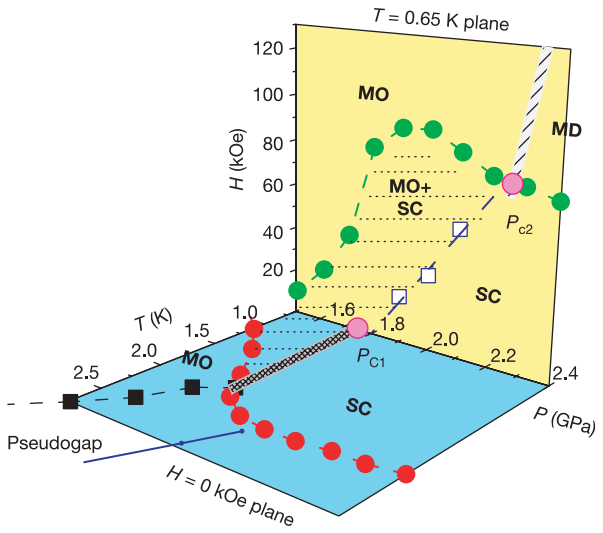

Figure 4 | The field–temperature–pressure phase diagram of the heavy fermion superconductor $CeRhIn_5$. The temperature–pressure plane is at $H = 0$ kOe and the H–P plane is for $T = 650$ mK. In the temperature–pressure plane, the magnetically ordered (MO) state of Ce 4*f* moments is preferred at low pressure. With increasing pressure, an SC phase appears and coexists with the MO phase when $P < 1.77$ GPa. For $1.77 < P < 2.3$ GPa, an SC phase is only found in zero field, but applied magnetic field induces a MO phase in the SC state. The blue line is a proposed pseudogap line[13]. In the H–P plane, upper critical fields H_{c2}, where superconductivity is totally depressed owing to the overlap of magnetic vortex cores, are represented by green circles. Quantum phase transitions between the pure SC phase and the coexistence phase of H-induced magnetism and SC are shown as open squares. The hatched grey line delineates a boundary between the MO phase and a magnetically disordered (MD) phase in the normal state. This boundary is defined by field-dependent specific heat and de Haas–van Alphen measurements, which were made at milliKelvin temperatures and fields $88 < H < 169$ kOe (ref. 16). P_{c1} is a quantum phase transition point between SC + MO and SC phases at zero magnetic field. P_{c2} is a tetracritical point where the H_{c2} line and the MO to MD lines cross. Experimental data constrain P_{c2} to within ± 0.05 GPa. The dashed line between P_{c1} and P_{c2} is a fit to the data as described in the text.

coexist at a quantum critical point[20]. This model, however, does not include the role of superconductivity.

Neutron-diffraction experiments also have revealed field-induced magnetic order in the superconducting state of the high-T_c compound $La_{1.9}Sr_{.1}CuO_4$ (ref. 21). Motivated by these observations, Demler and co-workers proposed a model that assumes the superconductor is near a quantum-phase transition to a state with microscopic coexistence of superconducting and magnetic orders[6,7]. When the magnetic field penetrates an unconventional superconductor in which the superconducting energy gap has nodes on the Fermi surface, field-induced quantized vortices have an AFM ground state that suppresses superconductivity around the vortices. The suppression of the superconducting order enhances the competing AFM order even outside of the normal vortex cores, thus delocalizing magnetic correlations and creating microscopic coexistence of the AFM and superconducting orders. Repulsive coupling between AFM and superconducting (SC) orders that can be tuned either by chemical substitution or pressure tips the balance between the two competing ground states, leading to a quantum phase transition among the pure AFM phase, the AFM + SC coexisting phase, and the pure SC phase. This model accounts for the evolution of magnetic order in $La_{1.9}Sr_{.1}CuO_4$ and its strengthening with increasing field[21].

This model[6,7] further predicts a line of quantum phase transitions between the AFM + SC and SC phases as a function of a control parameter δ. Taking pressure as the control parameter, this model predicts: $H/H^0_{c2} \approx 1 - \gamma[1 - \alpha(P-P_{c1})]$ for $H/H^0_{c2} > 0.1$, where H^0_{c2} is the upper critical field at a tetracritical point (P_{c2} in Fig. 4), γ is a numerical constant, and α is a proportionality between pressure and a repulsive coupling constant ($\delta = \alpha P$). A least-squares fit of this relationship to the open squares in Fig. 4 gives $\alpha = 1.99$, $\gamma = 1.11$, and $P_{c1} = 1.75$ GPa (dashed line in the field–pressure plane of Fig. 4). The numerical constant γ is in good agreement with that ($\gamma = 1.2$) obtained from a numerical solution of this model[7]. We also obtain P_{c2} ($H = H^0_{c2}$) = 2.25 GPa, which is very close to the pressure at which the effective mass of charge carriers diverges[16]. The H-linear proportionality of the magnetic entropy (Fig. 3a inset) and the microscopic coexistence of AFM and superconductivity in $CeRhIn_5$ are consistent with this model[6,7], which considers AFM order as the competing ground state of superconductivity. A possible explanation for the above phenomenological description of $CeRhIn_5$ is that the presence of superconductivity strongly inhibits a mechanism by which spins communicate, such as the Rudermann–Kittel–Kasuya–Yoshida (RRKY) interaction, which then may explain why magnetism is hidden in zero field by superconductivity when $T_c > T_N$.

Similarities between the high-T_c copper oxides[21–25] and $CeRhIn_5$ suggest that some phenomena they exhibit may be ubiquitous features of magnetically mediated superconductivity. The model of criticality that accounts for our data is not specific to the microscopic origin of unconventional superconductivity or of quantum criticality. Antiferromagnetism is due to localized 4*f*-electrons and quantum criticality is associated with a localized-to-delocalized transition in the 4*f*-configuration of $CeRhIn_5$, but this is not an appropriate description of copper oxide physics, nor possibly of all heavy-electron compounds. Consequently, within this model, the mechanism of unconventional superconductivity may differ in detail from system to system, even though magnetism is a common denominator.

Received 10 November 2005; accepted 2 January 2006.

1. Muller, K.-H. & Narozhnyi, V. N. Interaction of superconductivity and magnetism in borocarbide superconductors. *Rep. Prog. Phys.* **64,** 943–1008 (2001).
2. Moriya, T. & Ueda, K. Antiferromagnetic spin fluctuations and superconductivity. *Rep. Prog. Phys.* **66,** 1299–1341 (2003).
3. Curro, N. J. *et al.* Unconventional superconductivity in $PuCoGa_5$. *Nature* **434,** 622–625 (2005).
4. Coleman, P. & Schofield, A. J. Quantum criticality. *Nature* **433,** 226–229 (2005).
5. Mathur, N. D. *et al.* Magnetically mediated superconductivity in heavy fermion compounds. *Nature* **394,** 39–43 (1998).
6. Demler, E., Sachdev, S. & Zhang, Y. Spin-ordered quantum transitions of superconductors in a magnetic field. *Phys. Rev. Lett.* **87,** 067202 (2001).
7. Zhang, Y., Demler, E. & Sachdev, S. Competing orders in magnetic field: spin and charge order in the cuprate superconductors. *Phys. Rev. B* **66,** 094501 (2002).
8. Fujita, M. *et al.* Magnetic and superconducting phase diagram of electron-doped $Pr_{1-x}LaCe_xCuO_4$. *Phys. Rev. B* **67,** 014514 (2003).
9. Demler, E., Hanke, W. & Zhang, S.-C. SO(5) theory of antiferromagnetism and superconductivity. *Rev. Mod. Phys.* **76,** 909–974 (2004).
10. Lefebvre, S. *et al.* Mott transition, antiferromagnetism, and unconventional superconductivity in layered organic superconductors. *Phys. Rev. Lett.* **85,** 5420–5423 (2000).
11. Hegger, H. *et al.* Pressure-induced superconductivity in quasi-2D $CeRhIn_5$. *Phys. Rev. Lett.* **84,** 4986–4989 (2000).
12. Nicklas, M. *et al.* Two superconducting phases in $CeRh_{1-x}Ir_xIn_5$. *Phys. Rev. B* **70,** 020505R (2004).
13. Mito, T. *et al.* Coexistence of antiferromagnetism and superconductivity near the quantum criticality of the heavy-fermion compound $CeRhIn_5$. *Phys. Rev. Lett.* **90,** 077004 (2003).
14. Fisher, R. A. *et al.* Specific heat of $CeRhIn_5$: pressure-driven evolution of the ground state from antiferromagnetism to superconductivity. *Phys. Rev. B* **65,** 224509 (2002).
15. Llobet, A. *et al.* Magnetic structure of $CeRhIn_5$ as a function of pressure and temperature. *Phys. Rev. B* **69,** 024403 (2004).
16. Shishido, H. *et al.* A drastic change of the Fermi surface at a critical pressure in $CeRhIn_5$: dHvA study under pressure. *J. Phys. Soc. Jpn* **74,** 1103–1106 (2005).
17. Bao, W. *et al.* Incommensurate magnetic structure of $CeRhIn_5$. *Phys. Rev. B* **62,** R14621 (2000).

18. Cornelius, A. L. *et al.* Field-induced magnetic transitions in the quasi-two-dimensional heavy-fermion antiferromagnets Ce_nRhIn_{3n+2} (n = 1 or 2). *Phys. Rev. B* **64,** 144411 (2001).
19. Knebel, G. *et al.* High-pressure phase diagrams of $CeRhIn_5$ and $CeCoIn_5$ studied by ac calorimetry. *J. Phys. Condens. Matter* **16,** 8905–8922 (2004).
20. Si, Q. *et al.* Locally critical quantum phase transitions in strongly correlated metals. *Nature* **413,** 804–808 (2001).
21. Lake, B. *et al.* Antiferromagnetic order induced by an applied magnetic field in a high-temperature superconductor. *Nature* **415,** 299–302 (2002).
22. Lake, B. *et al.* Spins in the vortices of a high-temperature superconductor. *Science* **291,** 1759–1762 (2001).
23. Khaykovich, B. *et al.* Field-induced transition between magnetically disordered and ordered phases in underdoped $La_{2-x}Sr_xCuO_4$. *Phys. Rev. B* **71,** 220508R (2005).
24. Kang, H. J. *et al.* Antiferromagnetic order as the competing ground state in electron-doped $Nd_{1.85}Ce_{0.15}CuO_4$. *Nature* **423,** 522–525 (2003).
25. Panagopoulos, C. *et al.* Evidence for a generic quantum transition in high-T_c cuprates. *Phys. Rev. B* **66,** 064501 (2002).

Supplementary Information is linked to the online version of the paper at www.nature.com/nature.

Acknowledgements The authors thank Y. K. Bang, A. V. Balatsky and N. J. Curro for discussions. Work at Los Alamos National Laboratory was performed under the auspices of the United States Department of Energy Office of Science. H.Q.Y. acknowledges an ICAM postdoctoral fellowship.

Author Information Reprints and permissions information is available at npg.nature.com/reprintsandpermissions. The authors declare no competing financial interests. Correspondence and requests for materials should be addressed to T.P. (tuson@lanl.gov).